

REFLECTION OF SHOCK WAVES FROM A SOLID BOUNDARY IN A MIXTURE OF CONDENSED MATERIALS.

2. NONEQUILIBRIUM APPROXIMATION

A. A. Zhilin and A. V. Fedorov

UDC 532.529

The process of reflection of shock waves from a solid wall in a two-component mixture of condensed materials is numerically studied with account of the difference in velocities and pressures of the components within the framework of mechanics of heterogeneous media. It is shown that a shock wave (SW) of the dispersed type with monotonic velocity profiles can be reflected by an SW of a similar type with monotonic/nonmonotonic velocity profiles. A dispersed SW with a nonmonotonic velocity profile in the light component and a monotonic velocity profile in the heavy component is reflected by an SW of the dispersed-frozen type. When a frozen-dispersed SW is reflected, its type is either preserved, or changed to the dispersed-frozen structure depending on the initial parameters of the mixture. A dispersed-frozen SW is reflected by an SW of the same type with slight changes in the velocity and pressure profiles. A frozen SW of the two-front configuration can be reflected as an SW of the dispersed-frozen type or a frozen SW of the two-wave configuration. It is shown that a boundary layer is formed near the wall, where the volume concentration and the density of the light component exceed the corresponding values behind the reflected SW.

We discuss the results of numerical calculations of initial-boundary problems (1), (2) from [1] performed in the nonequilibrium approximation and studied within the framework of the equilibrium model. As in [1], all the quantities are presented in the dimensionless form.

First of all, we present some results [2–4] concerning possible types of shock waves interacting with the solid wall, which will be needed in what follows. Figure 1 shows a chart of solutions for the incident and reflected shock waves in the plane of the initial volume concentration m_{10} and SW velocity $|D|$ (we note that the equilibrium velocities $C_{e,0}$, $C_{e,fin}$, and C_{er} in this plane merge into one line C_e). In particular, the typical feature of the regions I_{11} and I_{12} is the presence of unstable flow in the form of a rarefaction shock wave, where $u_0 - D < u_{fin} - D$. In the regions I_{21} and I_{31} , the incident SW has a fully dispersed structure with either monotonic velocity profiles of the components, or a nonmonotonic velocity profile for the light component with a local minimum and a monotonically decreasing profile for the heavy component. In the regions I_{22} and I_{32} , the incident shock waves have monotonically decreasing velocity profiles in the heavy component. Concerning the light component, an SW of low amplitude has a monotonically decreasing velocity profile both in front of and behind the internal discontinuity, whereas for an SW with a higher amplitude, the velocity of the light component increases behind the discontinuity to the final equilibrium state. In the regions I_{41} and I_{51} , the incident shock waves have a bow SW in the second component supplemented by the relaxation zone, where the velocity decreases monotonically to the final equilibrium state, and a continuously decreasing

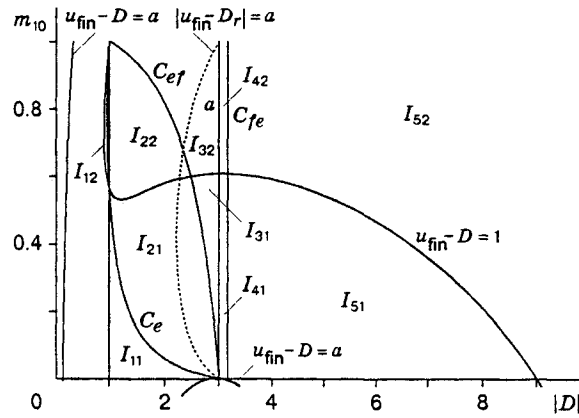


Fig. 1

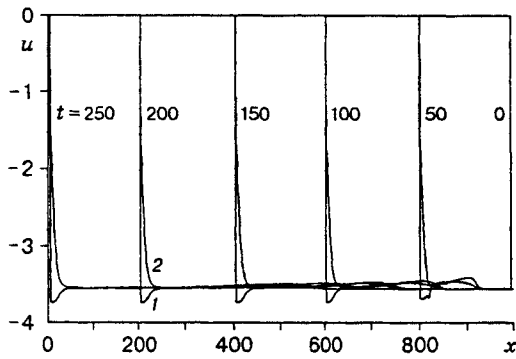


Fig. 2

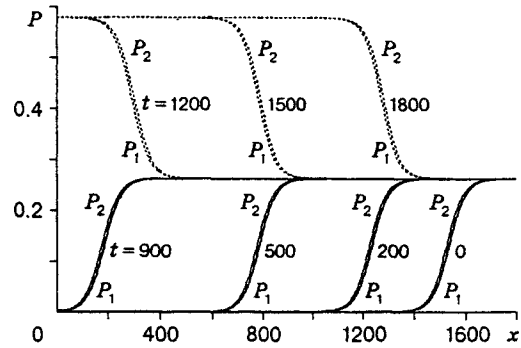


Fig. 3

velocity profile in the first component with an inflection at the point of incipience of the bow discontinuity. In the regions I_{42} and I_{52} , the incident shock waves have a two-wave configuration: the bow shock wave in the heavy component and the internal discontinuity in the light component. As the SW velocity increases, the distance between the bow and internal discontinuities decreases. Thus, for $D = -4$ and $m_{10} = 0.9$, the bow and internal shock waves practically merge and propagate together with a constant velocity. They correspond to curves 2 and 1 in Fig. 2.

For numerical calculations of initial-boundary problem (1), (2) from [1], we used a modified method of "coarse particles" [5]. The finite-difference equations for determining the velocities at the intermediate time layer with account of the buoyancy force, the expression for determining the volume concentration of the heavy component at the new time layer, and the stability conditions can be found in [6]; we also used the artificial viscosity introduced by Fedorenko [7].

1. We study SW reflection with initial parameters from the regions I_{21} and I_{31} . Here, for $D = -1.5$ and small m_{10} (see Fig. 1), the incident SW is fully dispersed and is reflected by an SW of the same type (the parameters of the mixture are such that the phase velocities and pressures do not differ much from each other). The parameters of the mixture for the incident and reflected SW were also close, i.e., $|D| \approx |D_r|$, $P_{fin} - P_0 \approx P_r - P_{fin}$. In numerical calculation, the reflected wave is formed and becomes steady almost immediately. The pressure profiles of the phases are plotted in Fig. 3 for $m_{10} = 0.2$ and $D = -1.5$. The velocity of the reflected SW for $D_r = 1.636$ (dashed curves) is slightly greater than the velocity of the incident wave for $D = -1.5$ (solid curves). There is no significant difference in the curvature of the velocity and pressure profiles for the incident and reflected shock waves; in regions adjacent to equilibrium states, the

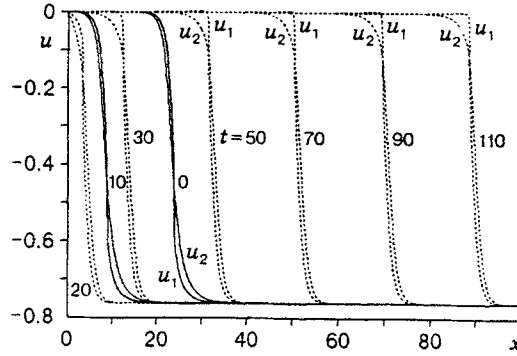


Fig. 4

incident wave is characterized by a smoother junction [cf. curves in Fig. 3 for $t = 500$ (incident SW) and 1500 (reflected SW)]. The configuration of the pressure profiles of the reflected SW is almost a “mirror image” of the corresponding profiles in the incident SW. Zhilin and Fedorov [1, Table 1] demonstrated that the excess pressure on the wall exceeds the pressure increment in the incident SW: $k = (P_r - P_0)/(P_{\text{fin}} - P_0) \approx 2$. Thus, for low volume concentrations of the light component, there is an analogy with the classical problem of gas dynamics on shock-wave reflection from the wall for the case of a perfect gas with constant heat capacities, where the amplification factor of the reflected wave k for a weak incident SW is equal to two, and the ratio of velocities is $D_r/D = -1$. It is known that, for strong shock waves, the velocity of the reflected SW is smaller than the velocity of the incident SW for $\gamma < 3$ and greater than the incident SW velocity for $\gamma > 3$. In a two-component mixture, a similar effect of the increase and decrease in the reflected SW velocity relative to the incident SW velocity can be reached by varying the initial volume concentration of the light component (see [1, Table 1]). Behind the incident SW front ($m_{20} = 0.8$), the volume concentration of the heavy component increases monotonically to $m_{2\text{fin}} = 0.833$ and continues to increase behind the reflected SW front to $m_{2r} = 0.860$. The volume concentration of the first component decreases in the incident SW and then in the reflected SW too. The densities of the components of the mixture increase monotonically both behind the incident and reflected shock waves. An analysis of numerical data on the structure of flow profiles for the incident and reflected shock waves showed that the width of the reflected SW is smaller by one third than the incident SW width. This is caused by amplification of the reflected SW [3].

We consider the reflection of a frozen-dispersed SW. The incident SW has an internal discontinuity in the flow parameters of the first component and a weak discontinuity in the second component (in the regions I_{22} and I_{32} in Fig. 1) at $m_{10} = 0.85$. The reflected SW belongs to the same class, but is characterized by a nonmonotonic behavior of velocity. It is seen in Fig. 4 that, for $D = -1.5$ and $m_{10} = 0.85$, the velocity of the light phase u_1 behind the reflected SW front is slightly greater than the final equilibrium value. This is explained by the fact that the reflected SW with D_r moves in the mixture with parameters corresponding to the new equilibrium state, and the final SW state in the chart of solutions (see Fig. 1) shifts toward higher velocities and lower volume concentrations. The calculation conducted using formula (3) (see [1]) showed that this state is characterized by reduced initial parameters $u'_0 = u_{\text{fin}} - D_r = -1.715$, $m'_{10} = m_{1,\text{fin}} = 0.712$, and $P'_0 = P_{\text{fin}} = 1.426$, and the reflected SW velocity is smaller than the incident SW velocity (see also [1, Fig. 1]).

An increase in m_{10} to 0.95 leads to an even greater decrease in the reflected SW velocity. The qualitative behavior of the velocity and pressure profiles for the incident ($u_0 - D = -1.5$ and $m_{10} = 0.95$) and reflected ($u_{\text{fin}} - D_r = -1.572$ and $m_{1,\text{fin}} = 0.896$) shock waves is identical.

We pay attention once again to the behavior of volume concentrations and densities of the mixture behind the reflected SW front. The volume concentrations of the components of the mixture on the solid wall and in the final equilibrium state behind the reflected SW front depending on the volume concentration

TABLE 1

*Steady Parameters of the Mixture on the Solid Wall
behind the Reflected SW Front for $D = -1.5$*

m_{10}	m_{2r}	m_{2r}^w	ρ_{1r}	ρ_{1r}^w	ρ_{2r}	ρ_{2r}^w
0.20	0.860	0.860	0.220	0.220	2.335	2.335
0.50	0.800	0.797	0.922	0.938	2.442	2.432
0.85	0.458	0.425	3.111	3.300	1.455	1.351
0.95	0.193	0.167	4.334	4.472	0.605	0.524

of the light component are listed in Table 1. It is seen that a boundary layer is formed in the region near the wall; the values of the volume concentration and density of the light component here exceed the final values behind the reflected SW, whereas these values for the heavy component are smaller than in a steady flow behind the reflected SW front.

We study in more detail the processes that occur near the solid wall upon transformation of an incident shock wave of the frozen-dispersed type into a reflected SW. The process of interaction of this SW with the wall can be conventionally divided into three stages. At the initial stage, the density and pressure of the components of the mixture smoothly increase, the volume concentration of the discrete component increases, and the volume of the carrier material decreases. This stage lasts until the internal SW approaches the wall. Then follows the stage of a jumplike increase in pressures and densities of the components, which is induced by the contact of the internal SW in the light component with the wall. The density and volume concentration of the heavy particles on the wall reach a local maximum. At this stage, the pressure on the wall in the heavy component is greater than the pressure in the light component (for example, by 70% for $m_{10} = 0.95$) and exceeds the value of the final equilibrium pressure behind the reflected SW (by 45%). A rapid increase in pressure on the wall generates a reflected SW moving in the opposite direction. Finally, the third stage includes a subsequent smooth equalization of pressures of the components to the final equilibrium state behind the reflected SW, which corresponds to the value determined analytically. The densities of the components of the mixture on the wall smoothly increase, and the density of the heavy particles on the wall ρ_{2r}^w remains lower than in the final equilibrium state behind the reflected SW front ρ_{2r} , whereas the density of the light material on the wall ρ_{1r}^w remains greater than the final steady value ρ_{1r} behind the reflected SW. The behavior of the volume concentrations of the components of the mixture m_{2r} and m_{2r}^w in the region near the wall is qualitatively similar to the behavior of the densities (see Table 1).

The behavior of the parameters described above is caused by the fact that, when the SW is reflected from a solid surface, the reflected particles of the heavy phase interact with the incident heavy particles and light binder. Being recoiled from the wall, the heavy particles prevent the motion of the incident particles to the wall. At the same time, the light material, having a smaller inert mass, flows around the heavy particles and penetrates into the near-wall region. This process leads to a decrease in density and volume concentration of the heavy particles discretely distributed over the volume near the wall and to an increase in volume concentration and density of the light component. We note that the pressures of the components of the mixture behind the reflected SW are gradually balanced and reach the final equilibrium values.

Figure 5 shows the distribution of the volume concentration of the heavy particles m_2 in the case of SW reflection from the solid wall for $D = -1.5$ and $m_{10} = 0.95$. The solid curves correspond to the incident shock waves, the dashed curves to the reflected shock waves, and the thick curve shows the profile at the moment of contact between the internal SW and the wall. The profile of the volume concentration of the second component of the incident SW at the initial time ($t = 0$) is monotonically increasing and has an inflection point at the point of emergence of the internal SW in the light component. This configuration steadily propagates far from the wall ($t = 5$). When the first stage of reflection begins ($t = 9$ and 10), the volume concentration of the particles on the wall smoothly increases. At the moment of SW contact with

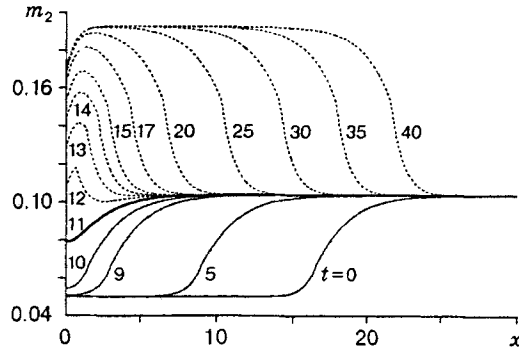


Fig. 5

the wall in the light component ($t = 11$), the point of weak discontinuity of the volume concentration of the heavy particles is also located on the wall. The value of m_2 on the wall is slightly higher than in the adjacent region, i.e., the point of a minimum shifts to the right from the wall. At the time $t = 12$, the reflected SW in the light component supported by the solid particles recoiled from the wall moves away from the wall, and the volume concentration of particles behind the SW front decreases. In the interval from $t = 13$ to $t = 30$, the volume concentration gradually increases to the final equilibrium value behind the reflected SW front, though it remains lower than the theoretical value near the wall. Then, at $t > 30$, the resultant flow with a weak discontinuity at the point of the internal shock wave in the light component steadily propagates over the mixture. Near the wall, the volume concentration of the particles retains a steady configuration whose profile smoothly decreases from $m_{2r} = 0.193$ to $m_{2r}^w = 0.167$ on the wall (see Table 1).

The above-considered problem of formation of an inhomogeneous layer in the vicinity of the solid wall is important in application problems of shock-wave loading of porous and mixture materials. One of the main requirements is the homogeneity of the final product. Nevertheless, experimental studies show that, in the process of shock-wave spraying of powders on a metal surface with oblique [8, 9] and normal [10] shock waves, macroscopic inhomogeneities are formed as an intermediate sublayer between the sprayed material and the sample surface. The structure and properties of this sublayer are significantly different from the structure and properties of the main material of the coating. In our case, this effect is caused by the formation of a small layer of the compressed light matter directly ahead of the solid wall.

2. We consider the reflection of a fully dispersed SW whose initial parameters are located in the regions I_{21} and I_{31} ($D = -2.5$) (see Fig. 1). For $m_{10} = 0.1$, the incident dispersed SW with monotonic profiles of velocities and pressures of the components is reflected as an SW with nonmonotonic velocity profiles in the light component. The pressures of the components remain monotonic.

For $m_{10} = 0.3$, the behavior of the flow parameters has a principally different character. The velocity decreases monotonically in the second component and has a minimum in the first component. The pressures increase monotonically within the entire flow region. When this structure is reflected, the type of the wave configuration is changed. The reflected SW has a bow shock wave in the second component and a monotonically increasing velocity profile in the first component, i.e., it is dispersed-frozen in our terminology. The pressures in the components of the mixture increase monotonically. We note that an internal equilibrium point in terms of the pressures of the components of the mixture appears. The pressure amplitude in the reflected SW increases almost by a factor of two as compared to the amplitude of the incident SW.

The increase in m_{10} to 0.5 also leads to a steady reflection of the dispersed-type SW: dispersed-frozen SW. As the initial volume concentration of the light component increases, the ratio of the pressure behind the reflected SW to the pressure behind the incident SW increases (see [1, Table 1]).

For $m_{10} = 0.7$ and $D = -2.5$, the incident frozen-dispersed SW (regions I_{22} and I_{32}) has an internal SW in the first phase and a continuous flow in the second phase, and the reflected wave is a frozen-dispersed

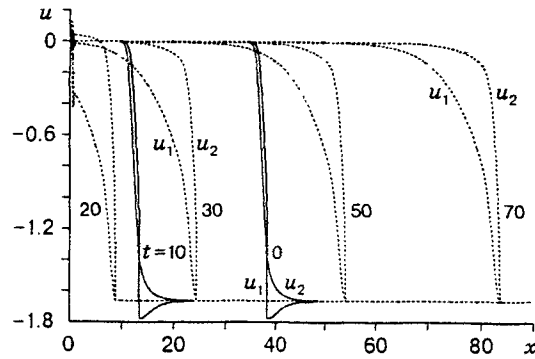


Fig. 6

SW with a bow discontinuity in the second component of the flow and a continuous flow in the first component (Fig. 6). In calculations, small perturbations of the solution appear in the near-wall region, since the strong incident and reflected shock waves interact there. As the amplitude of the incident SW increases ($m_{10} = 0.9$), the nonphysical oscillations of the flow in the near-wall region increase and a longer time is needed for flow stabilization behind the reflected SW. In the case $m_{10} = 0.9$, the reflected SW has no discontinuity in the second component, since $|u_{fin} - D_r| = -2.809 < a_2$ ($a_2 = 3$), and the monotonic velocity profile of the second component has a maximum whose value exceeds the velocity in the equilibrium state behind the reflected SW front.

3. In the regions I_{41} and I_{51} ($D = -3.3$), the incident and reflected shock waves have the dispersed-frozen type of flow at small values of m_{10} . When the SW is reflected, a flow of the same type with a nonmonotonic velocity profile in the first component arises, and the width of the relaxation zone increases, for example, almost by a factor of two at $m_{10} = 0.2$ and by a factor of three at $m_{10} = 0.4$. This effect is related to the fact that the volume concentration of liquid behind the incident SW dramatically decreases (almost by a factor of 6.7 at $m_{10} = 0.2$ and by a factor of 5.7 at $m_{10} = 0.4$), which affects the inertial properties of the materials of the mixture. Note that the SW amplitude in the second component also increases after reflection. The pressure profile for the incident SW in the first component has a monotonic, continuously increasing character; in the second component, it is nonmonotonic and has a maximum behind the bow shock wave. At the same time, the pressure profile of the reflected wave of the second component has a bow shock wave with a much greater amplitude and a wider relaxation zone. In the light component, the pressure profile remains monotonically increasing with a sharp growth in the head part of the reflected wave, and $P_1 < P_2$. In the region approaching the equilibrium state, P_1 is slightly greater than P_2 , i.e., there is an internal equilibrium point in terms of the pressures of the components.

A further increase in the initial volume concentration of the light component leads to the fact that the incident SW has a frozen two-front configuration, and the reflected SW has either a dispersed-frozen configuration for $m_{10} < m_{10}^*$, or a frozen two-wave configuration for $m_{10} > m_{10}^*$.

4. The conducted study allows the following conclusions.

After SW interaction with the wall, a layer of low density and volume concentration of the heavy particles is formed near the wall. As the SW amplitude (velocity) and initial volume concentration of the mixture near the wall increase, the degree of nonequilibrium relative to the final equilibrium state increases.

Depending on the incident SW velocity and volume concentration of the carrier phase, the type of the reflected SW can be the same as or different from the incident SW type. In particular,

- An incident SW of the dispersed type can be reflected as a dispersed or dispersed-frozen SW;
- A frozen-dispersed SW with a monotonically decreasing velocity profile is reflected as a frozen-dispersed SW with a monotonically decreasing or nonmonotonic velocity profile in the first component. A frozen-dispersed SW with a nonmonotonic velocity profile in the first component can be reflected as an SW

of a dispersed-frozen type with nonmonotonic velocity profiles of the components or of a dispersed type with a nonmonotonic velocity profile in the second component;

— A dispersed-frozen SW with the minimum value of the velocity of the first component is reflected as a dispersed-frozen SW with monotonic velocity profiles;

— A frozen SW of a two-front configuration can be reflected as a dispersed-frozen SW with monotonic velocity profiles and as a frozen SW of the two-front configuration.

REFERENCES

1. A. A. Zhilin and A. V. Fedorov, "Reflection of shock waves from a solid boundary in a mixture of condensed materials. 1. Equilibrium approximation," *Prikl. Mekh. Tekh. Fiz.*, **40**, No. 5, 73–78 (1999).
2. A. A. Zhilin, A. V. Fedorov, and V. M. Fomin, "Travelling wave in a two-velocity mixture of compressible media with different pressures," *Dokl. Ross. Akad. Nauk*, **350**, No. 2, 201–205 (1996).
3. A. A. Zhilin and A. V. Fedorov, "Shock-wave structure in a two-velocity mixture of compressible media with different pressures," *Prikl. Mekh. Tekh. Fiz.*, **39**, No. 2, 10–19 (1998).
4. A. A. Zhilin and A. V. Fedorov, "The shock-wave structure in a two-velocity mixture of compressible media with two pressures," in: *Proc. of the 8th Int. Conf. on the Methods of Aerophys. Research*, Vol. 2, Inst. Theor. and Appl. Mech., Novosibirsk (1996), pp. 237–242.
5. A. A. Gubaidullin, A. I. Ivandaev, and R. I. Nigmatulin, "Modified method of 'coarse particles' for calculation of unsteady wave processes in multiphase dispersed media," *Zh. Vychisl. Mat. Mat. Fiz.*, **17**, No. 6, 1531–1544 (1977).
6. A. A. Zhilin and A. V. Fedorov, "Propagation of shock waves in a two-phase mixture with different pressures of the components," *Prikl. Mekh. Tekh. Fiz.*, **40**, No. 1, 55–63 (1999).
7. R. P. Fedorenko, "Application of highly accurate difference schemes for numerical solution of hyperbolic equations," *Zh. Vychisl. Mat. Mat. Fiz.*, **2**, No. 6, 1122–1128 (1962).
8. N. A. Kostyukov and G. E. Kuz'min, "Criteria of occurrence of 'central-zone'-type macroinhomogeneities in the shock-wave loading of porous media," *Fiz. Goreniya Vzryva*, **22**, No. 5, 87–96 (1986).
9. V. Babul', Ya. Bagrovskii, and K. Berezhan'skii, "Explosive pressing of powders," *Fiz. Goreniya Vzryva*, **11**, No. 2, 259–264 (1975).
10. A. P. Alkhimov, S. V. Klinkov, V. F. Kosarev, and A. N. Papyrin, "Gas-dynamic spraying. Study of a plane supersonic two-phase jet," *Prikl. Mekh. Tekh. Fiz.*, **38**, No. 2, 176–183 (1997).